Journal Pre-proof

ADVANCED OCT ANALYSIS OF BIOPSY PROVEN VITREORETINAL LYMPHOMA

Francesco Pichi , Rosa Dolz-Marco , Jasmine H Francis , Adrian Au , Janet L Davis , Amani Fawzi , Sarra Gattousi , Debra A Goldstein , Pearse A Keane , Elisabetta Miserocchi , Alessandro Marchese , Kyoko Ohno-Matsui , Mandeep S Sagoo , Scott D Smith , Ethan K Sobol , Anastasia Tasiopoulou , Xialou Yang , Carol L Shields MD , K Bailey Freund , David Sarraf

PII: S0002-9394(21)00620-6
DOI: https://doi.org/10.1016/j.ajo.2021.11.023
Reference: AJOPHT 12084

To appear in: *American Journal of Ophthalmology*

Received date: August 10, 2021
Revised date: November 17, 2021
Accepted date: November 18, 2021

Please cite this article as: Francesco Pichi , Rosa Dolz-Marco , Jasmine H Francis , Adrian Au , Janet L Davis , Amani Fawzi , Sarra Gattousi , Debra A Goldstein , Pearse A Keane , Elisabetta Miserocchi , Alessandro Marchese , Kyoko Ohno-Matsui , Mandeep S Sagoo , Scott D Smith , Ethan K Sobol , Anastasia Tasiopoulou , Xialou Yang , Carol L Shields MD , K Bailey Freund , David Sarraf , ADVANCED OCT ANALYSIS OF BIOPSY PROVEN VITREORETINAL LYMPHOMA, *American Journal of Ophthalmology* (2021), doi: https://doi.org/10.1016/j.ajo.2021.11.023

TITLE: **ADVANCED OCT ANALYSIS OF BIOPSY PROVEN VITREORETINAL LYMPHOMA**

Short Title: **OCT findings in vitreo-retinal lymphoma**

Francesco Pichi[1,2]; Rosa Dolz-Marco[3]; Jasmine H Francis[4,5]; Adrian Au[6];Janet L Davis[7]; Amani Fawzi[8];Sarra Gattousi[9,01]; Debra A Goldstein[8]; Pearse A Keane[11]; Elisabetta Miserocchi[12]; Alessandro Marchese[13];Kyoko Ohno-Matsui[13]; Mandeep S Sagoo[,11,14]; Scott D Smith[1,2]; Ethan K Sobol[4,5]; Anastasia Tasiopoulou[11]; Xialou Yang[15]; Carol L Shields MD[15]; K Bailey Freund[16,17]; David Sarraf[6,18]

[1]Cleveland Clinic Abu Dhabi, Eye Institute, Abu Dhabi, United Arab Emirates

[2]Cleveland Clinic Lerner College of Medicine, Case Western Reserve University, Cleveland, USA

[3]Unit of Macula, Oftalvist Clinic, Valencia, Spain

[4]Ophthalmic Oncology Service, Memorial Sloan Kettering Cancer Center, New York, NY, USA

[5]Department of Ophthalmology, Weill Cornell Medical Center, New York, NY, USA

[6]Stein Eye Institute, University of California, Los Angeles, Los Angeles, California (USA)

[7]Bascom Palmer Eye Institute, University of Miami-Miller School of Medicine, Miami, Florida (USA)

[8]Department of Ophthalmology, Northwestern University Feinberg School of Medicine, Chicago, Illinois, USA

[9]University Bordeaux, Inserm, Bordeaux Population Health Research Center, LEHA Team, Bordeaux, France

[10]Department of Ophthalmology, Bordeaux University Hospital, Bordeaux, France

[11]NIHR Biomedical Research Centre at Moorfields Eye Hospital NHS Foundation Trust and UCL Institute of Ophthalmology, London, UK

[12]Uveitis Service, department of Ophthalmology, IRCCS, San Raffaele Scientific Institute, Milan, Italy

[13]Department of Ophthalmology and Visual Science, Tokyo Medical and Dental University, Tokyo, Japan

[14]Ocular Oncology Service, Moorfields Eye Hospital, London, UK

[15]Ocular Oncology Service, Wills Eye Hospital, Thomas Jefferson University, Philadelphia, Pennsylvania, USA

[16]Vitreous Retina Macula Consultants of New York, New York, New York

[17]Department of Ophthalmology, NYU Grossman School of Medicine, New York, New York

[18]Greater Los Angeles VA Healthcare Center, Los Angeles, California (USA)

Corresponding Author

Francesco Pichi MD

Cleveland Clinic Abu Dhabi

PO Box 112412

Abu Dhabi, United Arab Emirates

Email: ilmiticopicchio@gmail.com

Mobile: +971559176234

ABSTRACT

Importance: Although the diagnosis of vitreoretinal lymphoma (VRL) can be challenging, early detection is critical for visual prognosis.

Objective: To analyze the spectrum of optical coherence tomography (OCT) findings in patients with biopsy-proven VRL and correlate these features with clinical parameters.

Design: Retrospective cross-sectional study

Setting Multicenter chart review from 13 retina, uveitis and ocular oncology clinics worldwide over an 11-year period (2008-2019).

Participants: Patients with a diagnosis of biopsy-proven VRL imaged with OCT at presentation

Exposure: The ocular information, systemic information and multimodal retinal imaging findings were collected and studied.

Main Outcome Measure Characteristics of VRL on OCT

Results A total of 182 eyes of 115 patients (63 women, mean age 65 years) were included in this study. The disease was bilateral in 81 (70%) patients, and mean baseline visual acuity (VA) was 0.2±0.89 logMAR (Snellen equivalent of 20/32). At baseline, 38 patients (33%) presented with isolated ocular involvement, 54 (45%) with associated central nervous system (CNS) involvement and 11 (10%) with other systemic lymphomatous involvement and an additional 12 (10%) patients presented with both CNS and other systemic involvement. On OCT, tumor infiltration was identified in various retinal layers including lesions in the sub-retinal pigment epithelium (RPE) compartment (91% of eyes), the subretinal compartment (43% of eyes) and the intraretinal compartment (7% of eyes).

Conclusions and Relevance OCT analysis of eyes with vitreoretinal lymphoma identified 3 main regions of retinal infiltration. Sub-RPE location, with or without subretinal infiltration, was the most common pattern of involvement whereas isolated intraretinal infiltration was the least common.

Introduction

Vitreoretinal lymphoma (VRL) is strongly associated with primary central nervous system (CNS) lymphoma[1,2] and is the most prevalent and aggressive extranodal presentation of non-Hodgkin's lymphoma. Histopathologically, the cells are of diffuse large B-lymphocyte origin in 80% of cases.[3] Ocular involvement in VRL can be primarily diagnosed in the eye, concurrent with or follow CNS lymphoma diagnosis.[4] Patients diagnosed with CNS lymphoma develop ocular involvement in 15–25% of cases[5-9]. In lymphoma primarily diagnosed in the eye, 16-34% of patients will have CNS involvement at ocular diagnosis[10,11] while 65%–90% of the remainder will eventually develop CNS manifestations, usually within 2-3 years.[4,5] Overall, between 35% and 90% of VRL patients show evidence of CNS lymphoma at some point during the course of disease.

VRL typically occurs in older patients with a median age of 60 years[12-14]. High mortality is due to CNS lymphoma, which has a mean survival of 32 months[3] and a 5-year survival rate of 61%.[15] Although early detection is critical, the diagnosis of VRL can be challenging.[3] VRL represents less than 0.01% of all vitreoretinal diagnoses, and therefore may not be considered in the initial differential diagnosis.[2,16] The clinical findings are considered non-specific but can lead to vision loss and even blindness. VRL can masquerade as a posterior or intermediate uveitis that may initially be responsive to local and systemic corticosteroid, but recurs with prolonged corticosteroid treatment.[17-19]

Due to its propensity to mimic other ocular diseases, VRL is considered a masquerade syndrome. At tertiary referral centers, VRL has been reported to comprise 33% of all masquerade syndromes, 81% of neoplastic masquerades, and approximately 2% of all uveitis referrals.[20,21] The classic ophthalmoscopic presentation includes vitreous cells with multiple placoid yellow-white sub-retinal pigment epithelium (RPE) infiltrates, and RPE alterations including a leopard-spot pattern.[22,23]. However, these fundus findings occur in only about 40% of patients.[24] While macular edema is not a typical finding in VRL, intraretinal fluid has been identified in some studies.[24-28] Other reported clinical findings include cells in the aqueous humor[29] and sheets of vitreous cells associated with retinal phlebitis.[30]

Non-invasive imaging modalities such as optical coherence tomography (OCT) have previously demonstrated the capability to display characteristic findings of VRL, although this evidence is largely limited to case reports or small case series [23,31-37] including cases following treatment where the diagnosis of VRL was already made.[38] While such modalities have been proposed to enable earlier identification of VRL and may reduce the dependence on invasive biopsy, there are few OCT studies investigating the morphologic features of VRL and the correlation with ocular and systemic findings. Furthermore, earlier diagnosis informed by increased awareness of the OCT findings of this entity can enable earlier treatment, which in turn, has potential to reduce ocular morbidity and systemic mortality.

The aim of this study was to analyze a large series of pretreatment OCT images from patients with biopsy-proven VRL and to describe the spectrum of OCT features in the early and late stages of the disease as well as correlate these OCT findings with clinical data and outcomes.

Materials and Methods

Institutional Review Board approval was determined by the respective coauthors according to the requirements established by their institutional centers. The study adhered to the principles set forth by the Declaration of Helsinki.

At each institution, patients with the diagnosis of VRL were identified through a retrospective review of medical records from 2008 to 2019. Inclusion criteria for the analysis included: 1) VRL identified on the basis of either positive ocular tissue biopsy including vitreous cytologic analysis or positive CNS tissue biopsy, 2) gradable baseline OCT raster scans through lymphomatous lesions, whether in the macula or extramacular, and 3) high quality color fundus photographs. De-identified patient records and multimodal imaging (MMI) data from the baseline and subsequent examinations were collected and reviewed.

Baseline and final follow-up Snellen visual acuity (VA) were recorded and converted to logarithm of the minimal angle of resolution (LogMAR) values. Visual acuities of count fingers, hand motion, light perception, and no light perception vision were assigned LogMAR

designations of 1.7, 2.0, 2.3, and 3.0, respectively. Biomicroscopic examination information were recorded as well as dilated fundus exam findings to determine the location of the lymphomatous lesions (macular, extramacular or a combination of both). Additional information collected from the medical record included the following: patient demographics including age, gender, and race; symptoms at baseline; time between presentation and definitive diagnosis of lymphoma; details regarding the investigational work-up including the surgical procedures required for diagnosis; methods of histopathologic and molecular diagnosis; time from diagnosis of VRL to CNS involvement; and the list of ocular and systemic treatments received. Medical records were reviewed to determine any evidence of CNS or non-CNS systemic involvement, and the time interval from presentation to CNS or non-CNS systemic progression was also evaluated. The term "VRL" was adopted for all modes of presentation where the main affected compartments did not affect the choroid on imaging with OCT. Clinical features at baseline ocular examination, including the pattern of retinal involvement (subretinal or intraretinal) were also recorded.

Baseline pretreatment OCT raster scans were independently assessed by two masked observers (FP and RDM) for the presence of sub-RPE, subretinal, and intraretinal hyperreflective material, and for the presence of subretinal or intraretinal fluid. These OCT findings were reviewed with the senior author (DS) and correlated with the systemic and CNS findings.

Color fundus photographs and widefield multicolor fundus images were analyzed for the presence of vitreous haze, mass lesions, areas of atrophy, and RPE alterations. The optic nerve head was analyzed for the presence of peripapillary hemorrhages or blurred margins suggestive of lymphomatous involvement of the optic nerve. When available, fundus autofluorescence (FAF) images were evaluated for patterns of abnormal hyperautofluorescence or hypoautofluorescence, including a "leopard spot" pattern defined as hyperautofluorescent spots ranging from 50 um to 250 μm in diameter alternating with adjacent hypoautofluorescent spots in the posterior pole and/or periphery. Hypoautofluorescence due to blockage was defined as RPE autofluorescence masked by a subretinal infiltrate. Hyperautofluorescence was defined as multiple hyperautofluorescent spots corresponding to areas of outer retinal disruption, more readily identifiable on FAF than on fundus photography.[40] When available, fluorescein

angiography (FA) findings were evaluated for the presence of a leopard spot pattern showing granular areas of hyperfluorescence intermixed with hypofluorescence, areas of hyperfluorescent window defects due to RPE loss, regions of RPE mottling with late staining, and hyperfluorescent foci or areas of dye leakage and/or dye pooling. Leakage of the optic nerve head was also assessed to identify optic nerve swelling and involvement.

Statistical analysis was completed using Stata 13.1 statistical software (StataCorp, College Station, TX). Two-group comparison of continuous variables was performed using the *t*-test for comparison of mean values. Visual outcome across multiple groups was analyzed by comparing mean values of baseline and change in logMAR VA using one-way analysis of variance with the Bonferroni correction for multiple comparisons. Categorical variables were analyzed by comparison of proportions using Fisher's exact test. Hypothesis testing used two-tailed statistics and significance was defined by $p \leq 0.05$.

Results

In this analysis, there were 152 patients with a diagnosis of VRL affecting 256 eyes**.** There were 23 patients (15%) excluded due to lack of tissue diagnosis for VRL. Of the remaining 129 patients (235 eyes), the diagnosis of VRL was based on vitreous cytologic findings in 94 patients (73%), chorioretinal biopsy in 11 patients (8%), a combination of vitreous and chorioretinal biopsy in 14 patients (11%), and brain biopsy and/or cerebrospinal fluid cytologic findings in 10 patients (8%) of which only 3 eyes (1%) also had a vitreous biopsy. Aqueous humor analysis of IL-10 and IL-6 was performed in 34 patients (26%) and the IL-10/IL-6 concentration ratio was greater than 1 in 100% of cases; however, this was not considered an inclusion criterion for diagnosis of VRL.

Of the 235 eyes from 129 patients with biopsy proven VRL, high quality, baseline OCT raster scans through lymphomatous lesions were available for 182 eyes (77%) of 115 patients. Of these 115 patients, 63 (55%) were women and 52 (45%) were men. The mean age at baseline presentation was 64.73±10.86 (25-91) years and 67 of the 115 patients (58%) exhibited bilateral disease at baseline (Table 1). Mean baseline VA of this final cohort of 182 eyes was 0.2±0.89 logMAR (Snellen equivalent: 20/30).

Of the 115 patients that met both the tissue diagnostic and OCT inclusion criteria, 38 (33%) presented with vitreoretinal lymphoma, of whom 21 had bilateral disease. Fifty-four (47%) patients (33 with bilateral ocular disease) presented with a concomitant diagnosis of CNS lymphoma. Of these, 11 (10%) were diagnosed with CNS lymphoma before ocular involvement. Eleven patients (10%) (6 bilateral) presented with a concomitant history of non-CNS systemic lymphoma and in 4 of these 11 patients (3%) the diagnosis preceded the eye involvement. An additional 12 patients (10%, 7 patients with bilateral involvement) presented with both CNS and non-CNS systemic involvement.

Among the 182 eyes of 115 patients included in the analysis, the earliest available (baseline) OCT volume scan was analyzed, prior to tissue diagnosis, and before any lymphoma-specific treatments. Of these 182 eyes, 124 (68%) showed a combination of both macular and extramacular manifestations, 45 (25%) displayed macular changes alone, and 13 (7%) exhibited extramacular findings alone. From the 13 patients with only extramacular manifestations, peripheral OCT scans were available in all cases. Hyperreflective lesions were observed across multiple retinal layers as summarized in Figure 1 and Table 1.

Sub-retinal pigment epithelium (sub-RPE) infiltrates associated with thickening or detachment of the RPE were observed in 165/182 eyes (64%) (Figure 2A, 2B and 2C). Sub-RPE material was further classified into 3 categories (Table 1): 1. “Thickened RPE” (defined as the presence of thickening of the RPE/Bruch’s membrane (RPR/BrM) complex without a distinct separation between RPE and Bruch’s membrane; Figure 2A). 2. “Shallow RPE detachment or PED” (defined as a separation between RPE and Bruch’s membrane due to hyperreflective material, with a maximal PED height less than 250 µm; Figure 2B). 3. “Large PED” (defined as a dome-shaped PED with a maximal height greater than 250 µm showing anterior hyperreflective material posterior hyporeflective shadowing closer to Bruch’s membrane; Figure 2C). The most common sub-RPE feature was a “thickened RPE” (89 eyes, 49%), while “shallow” and “large” PEDs were less common (39 eyes [21%] and 37 eyes [20%], respectively).

Subretinal hyperreflective material (Figure 2D, 2E and 2F) was the second most common finding with OCT and was detected in 79/182 (43%) eyes (Table 1). These hyperreflective subretinal infiltrates often appeared as broad or band-like shallow lesions (Figure 2D), but others were more focal and more round in morphology (Figure 2E). Cloudy vitelliform lesions[39], defined as a macular detachment due to thick hyperreflective subretinal material resembling an acquired vitelliform lesion above an irregularly thickened or rippled RPE/BrM complex, was detected in 16/182 eyes (9%) (Figure 3A and 3C).

Twelve eyes (7%) exhibited intraretinal hyperreflective lesions extending from the outer nuclear layer as far as the nerve fiber layer (NFL) (Figure 2G, 2H and 2I).

The number of eyes showing various combinations of sub-RPE, subretinal, and intraretinal involvement is displayed in Figure 1. Sub-RPE lesions were present in isolation or in combination with subretinal and/or intraretinal lesions in 91% (165/182) of eyes in this study. Isolated sub-RPE (101/182 or 55%) and combined sub-RPE and subretinal (53/182, 29%) involvement were the most common baseline OCT features identified. Of note, 5% of eyes (10/182) displayed hyperreflective material in all 3 locations (sub-RPE, subretinal and intraretinal) and only 1 eye (0.5%) showed isolated intraretinal hyperreflective lesions (Figure 1). Of the 3 sub-categories of RPE involvement, no statistical difference was noted between eyes with “thickened RPE” and “shallow RPE detachment” regarding the presence of associated subretinal material (25% and 18%, *P*=0.1). By contrast, few eyes with “large RPE detachments” showed hyperreflective material in the subretinal space (3%) (Figure 2C).

An analysis of OCT features based on age did not show any statistical difference in age of patients with sub-RPE, subretinal and intraretinal lesions (mean age 65, 58 and 61 years, respectively, *P*=0.3). However, a sub-group analysis within the sub-RPE group showed that patients with “large RPE detachment” on OCT were significantly older compared to the other groups (78 years, $P = 0.05$).

Intraretinal fluid (IRF) was observed in 23/182 eyes (13%) (Figure 4A and 4C) and subretinal fluid (SRF) in 20/182 eyes (11%) (Figure 4B and 4D). Ten eyes (5%) displayed a combination of

both IRF and SRF (Figure 4C). The presence of SRF was more commonly associated with sub-RPE material (18/20 eyes, 90%) (Figure 4B, 4C and 4D) and in particular with "large RPE detachments" (16/18 eyes, 89%; *P*>0.001) (Figure 4C and 4D). Conversely, IRF was more commonly associated with subretinal material (14/23 eyes, 61%) but this difference was not statistically significant (*P* = 0.1).

Mean baseline VA for the 182 eyes was 0.2±0.89 logMAR (Snellen equivalent: 20/30). An analysis of baseline VA according to OCT features showed that patients with a combination of subretinal and intraretinal material at baseline presented with the worst VA (1.30±1.41 logMAR, 20/400 Snellen), followed by patients with combined sub-RPE, subretinal and intraretinal material (0.96±0.88 logMAR, 20/200 Snellen) and patients with subretinal material alone (0.62±0.62 logMAR, 20/80 Snellen) or in combination with sub-RPE material (0.64±0.50 logMAR, 20/80 Snellen). The absence of hyperreflective material in the macula or the presence of only sub-RPE lesions at baseline was associated with relatively preserved VA (0.33±0.56 logMAR [20/40 Snellen] and 0.24±0.37 logMAR [20/30 Snellen], respectively).

Baseline color and/or multicolor fundus photographs (Figure 5A, 5E and 5I) were available for all 182 eyes. Notable fundus photographic findings included vitritis in 101 eyes (55%), subretinal lesions in 148 eyes (81%; Figure 5E AND I), retinal hemorrhage in 4 eyes (2%), leopard spotting in 17 eyes (9%; Figure 7E) and optic nerve head edema in 6 eyes (3%).

Fundus autofluorescence images were available for 162/182 (89%) eyes. Abnormal autofluorescence on FAF was identified in 89 eyes (55% of the 162 eyes). A leopard spot hyperautofluorescence (hyperAF) pattern was present in 61 eyes (33%) and was observed in various locations in the retina (Figure 5F) and was not limited to the location of the large subretinal infiltrates. A correlation of hyperAF with OCT patterns showed a higher association of the leopard spotting with the "thickened RPE" pattern (49/61 eyes, *P* = 0.05) and with "large RPE detachments" (12/61 eyes) (Figure 5B-D). Nine eyes (5%) showed a pattern of hyperAF associated in 100% of cases with a focal disruption of the ellipsoid zone on OCT. Sixteen eyes (9%) showed diffuse subretinal hyperAF of mild intensity in the macular area corresponding to a cloudy vitelliform OCT pattern (Figure 3C) and in 4 eyes (2%) the areas of diffuse hyperAF corresponded to "large RPE detachments" on OCT. HypoAF blockage by lymphomatous mass

lesions was noted in 5 eyes (3%) with “shallow RPE detachments” (Figure 5J) while hypoAF from RPE atrophy was noted in 7 eyes (4%).

Fluorescein angiography was available for 60 eyes (33%). Twenty-five eyes (15%) displayed a leopard spot pattern with a granular appearance. Seventeen eyes (10%) showed late hyperfluorescent staining of the lymphomatous lesions, 1 eye (1%) illustrated hyperfluorescence with well-defined borders suggestive of pooling and 2 eyes (1%) displayed early blockage with late staining of mass lesions. In 15 eyes (9%) of patients with vitritis alone, ultra-widefield FA demonstrated vascular leakage along medium and small retinal vessels in all 15 eyes. Petaloid macular leakage i.e. cystoid macular edema was not identified in any eyes of our series.

Despite the cross-sectional nature of this study, we briefly report the follow-up OCT analysis that was available for 42 of the enrolled 182 eyes (23.08%) and illustrated persistent retinal lesions in 7 eyes (17%, 4% of the 182 eyes), resolution of all retinal lesions in 17 eyes (40%, 9% of the 182 eyes) and resolution of all retinal lesions associated with atrophy of the outer retina in 18 eyes (43%, 10% of total).

Discussion

The diagnosis of VRL is a notoriously challenging task as the baseline presentation can masquerade as an inflammatory or infectious posterior uveitis. Given the challenges of clinical diagnosis, a number of immunological analyses have been proposed using either vitreous or aqueous fluid, with diagnosis supported by the presence of B-lymphocyte biomarkers such as an elevated IL-10:IL-6 ratio versus the usual T-lymphocyte-derived mediators. Such analyses are only possible with highly differentiated malignancies and may be limited by the development of a T-lymphocyte driven response to tumor antigens. Definitive diagnosis of VRL is made by vitreous and/or chorioretinal biopsy, often in conjunction with flow cytometry and cytology analysis. However, cytology specimens obtained through vitreoretinal biopsy have been shown to generate false negative results in approximately 30% to 45% of analyses.[1,31]Vitreous samples are often insufficient with low cellular yield and results can be challenging to interpret unless the

pathologist has prior experience in the diagnosis of VRL. Furthermore, cytology samples degrade rapidly unless suitably fixed, rendering results inaccurate unless promptly analyzed.[13] Molecular testing for the presence of MYD88 mutations may enhance diagnosis of VRL. [32,33,] Definitive diagnosis requires tissue biopsy. However, advancements in multimodal imaging can now provide an avenue to enhance identification of features of this elusive disease and characteristic patterns suggestive of VRL can be identified with OCT, FAF, and FA. Early suspicion and detection of the ocular disease may be aided by a greater appreciation of the spectrum of clinical findings of OCT.

OCT provides the capability to easily and rapidly acquire images that are reproducible and readily interpreted. In our series of 182 biopsy proven VRL, SD-OCT showed a preponderance of isolated hyperreflective deposits in the sub-RPE space (55%), followed by a combination of the same in the sub-RPE and subretinal space (29%). Isolated subretinal deposits were less commonly identified (9%) and intraretinal deposits extremely rare (0.5%).
Despite the power to detect a spectrum of significant pathological findings, there can be significant overlap of morphological features with other diseases including posterior uveitis, age-related macular degeneration, and even diabetic retinopathy. Isolated extra-macular lesions were present in less than 10% of eyes on dilated fundus in this study, indicating the importance of macular OCT as a modality to enhance early detection and diagnosis of VRL. Further OCT was successfully performed in 100% of the extramacular lesions.

Our study included the largest number of biopsy proven VRL cases captured and analyzed with OCT with relatively early findings of VRL before definitive tissue diagnosis and ocular and systemic therapy. In a recent publication, Barry et al[40] described the OCT findings of VRL in a cohort of 22 patients and noted hyperreflective nodules in the sub-RPE and in the subretinal space in 16% and 53%, respectively. Casady et al[41] noted a higher incidence of sub-RPE deposits (43%) in 18 eyes with biopsy confirmed VRL. In a recent OCT study[42] of 55 eyes with VRL, RPE abnormalities (64%) and sub-RPE deposits (64%) were the most common finding and were isolated in 11% of eyes. Intraretinal and subretinal deposits were never detected as an isolated OCT finding but always in combination with other OCT features (in 15% and 36% of eyes, respectively).

In our series of 115 patients (182 eyes), sub-RPE lymphomatous infiltrates were the most common OCT finding (91%). Autopsy eyes have demonstrated that lymphoma cells in VRL typically reside between the RPE and Bruch's membrane.[12] Isolated sub-RPE lesions or in combination with subretinal lesions represented the most common baseline presentation (85%) in our study. By contrast, a baseline presentation that included infiltrates in sub-RPE, subretinal and intraretinal locations was identified in only 5% of eyes. Intraretinal lesions were rarely encountered and almost never occurred without associated sub-RPE infiltration.

There remains uncertainty about the pathophysiology of VRL. Our understanding of VRL is increasing, but because of the rarity of the disease and the difficulty in obtaining diagnostic tissue specimens, most of our knowledge is derived from studies in patients with primary CNS lymphoma. The origin of the abnormal lymphocytes and the mechanisms that guide the targeting of specific tissues have not been elucidated.[2,4,11] Whether the lymphoma cells originate from the retinal circulation or from the choroid through Bruch's membrane and the RPE remains controversial.[1] Only eight cases of VRL with immunohistopathologic analysis are reported in the literature.[43-47] Three of these cases illustrated localization of diffuse B-cell lymphoma cells only within the subretinal space.[44,45] Two cases showed that the majority of the cells were located within the subretinal space with a few B-cells identified within the choroid.[46,46] Finally, three cases demonstrated clear evidence of lymphocytes within the choroid.[43,44]

Deak et al[48] were the first to describe with OCT vertical hyperreflective lesions extending from the inner layers of the retina (GCL and RNFL) to the RPE in 5/7 patients with VRL and concomitant non-CNS or CNS systemic lymphoma and therefore proposed a retinal vascular origin for VRL which is a pathway supported by many experts in the uveitis field. Our OCT findings suggest a possible progression of lymphoma cells from the choroidal vasculature across the RPE and into the sub-RPE and subretinal space with final extension into the retina and vitreous. But this hypothesis needs to be validated with a prospective longitudinal OCT analysis. The main support for a choroidal origin is the presence of B-cell chemokines present on RPE cells.[49] In a seminal study, Chan et al[49] demonstrated that RPE cells expressed chemokines (BLC, SDF-1) in high levels. These chemokines bind to receptors highly expressed in B-cell

lymphomas (CXCR4, and CXCR5) and are not found anywhere else in the retina. In these 3 autopsy cases of PVRL, lymphoma cells were located between the RPE and the choroid; therefore, the Authors postulated that B-cell chemokines secreted by the RPE may attract lymphoma cells from the choroidal circulation.

The possibility that lymphoma cells started in the retinal vasculature and then migrated to and proliferated in the sub-RPE space is still plausible. However, this hypothesis would require that the endothelium of the retinal vasculature, the ELM, and the RPE tight junctions are leaky enough to allow a lymphoma cell to reach the sub-RPE space. In contrast, the choroidal origin of the B cells requires only Bruch's membrane tight junction to be disrupted.

There were additional OCT findings of interest in this study. Various forms of RPE involvement were identified including RPE thickening versus detachment. "Large RPE detachments" of hyperreflective lymphomatous material were associated with an older age (78.2 years, $P = 0.05$) and were frequently isolated lesions. Only rarely were large RPE detachments associated with hyperreflective material in the subretinal space (3% of total eyes in the study). Gass[48] has hypothesized that the RPE is more adherent to the underlying Bruch's membrane in younger patients compared to older patients, based on studies with macular neovascularization. This may explain the propensity for large PEDs to develop in the older patients of our study in which the lymphomatous infiltrates can more easily establish a plane for growth and extension as opposed to younger eyes in which the lesions are more likely to break through the RPE into the subretinal space because of greater adhesion of the RPE-BM complex. Furthermore, "large RPE detachments" strongly correlated ($P>0.001$) with OCT detection of pockets of SRF (Figure 4B and 4D) that may be secondary to impairment of the RPE pumping capacity when the RPE is further displaced from the underlying choroid which is the primary oxygen provider of the RPE.[50,51]

The cloudy vitelliform appearance of lymphomatous infiltration described by Pang et al[39] in 3 patients and reported by Barry et al[43] in 31.3% of their cases is now widely recognized as highly suggestive of VRL. We identified this characteristic central finding in only 9% of our patients. However, more subtle patterns of round or band-like hyperreflectivity in the subretinal space was a common finding and was noted in 43% of eyes in this study.

This series provides considerable support for the use of OCT as an aid to identify characteristic features of VRL, with the potential to positively influence patient outcomes. However, the conclusions we have drawn may be limited by the retrospective analysis and uncontrolled methodology of the study. In addition, ascertainment bias associated with tertiary care referrals may have confounded our analysis. It is possible that our cohort of VRL cases may represent a more advanced or severe process that is not representative of the general population of VRL cases in the community. Furthermore, due to the retrospective and multicenter nature of the study, there was a lack of uniformity in imaging modalities used to analyze the lymphomatous lesions. For example, the OCT analyses were largely limited to the macula, thus some extramacular lesions may have been missed.

We cannot say that our findings improve patient outcomes or increase the likelihood of pretest or pre biopsy probability. However we believe that this paper will help practitioners to better identify VRL and will enhance diagnosis and may ultimately increase the yield of tissue diagnosis but this awaits further validation correlating oct with tissue diagnosis yield.

Strengths of the study included the relatively large dataset of VRL cases that were all biopsy confirmed and all imaged with high resolution spectral domain OCT prior to VRL treatment.

In summary, the present study analyzed 115 patients and 182 eyes with biopsy confirmed vitreoretinal lymphoma and illustrated 3 main lesion types with OCT: sub-RPE, subretinal and intraretinal infiltrates. Isolated sub-RPE infiltration or a combination of sub-RPE and subretinal infiltration were the most common patterns of baseline presentation. Intraretinal infiltration was uncommon and almost never occurred without associated sub-RPE infiltration. While diagnosis of VRL cannot prescind from tissue analysis, these findings may point clinicians towards an early detection. Spectral domain OCT , a commonly used office tool with rapid acquisition and readily interpretable image analysis, may enhance the identification of lymphomatous infiltrates.

Table of contents

In this series of 182 biopsy proven vitreo-retinal lymphomas, SD-OCT showed a preponderance of isolated hyperreflective deposits in the sub-RPE space, followed by a combination of the same

in the sub-RPE and subretinal space. Isolated subretinal and intraretinal deposits were extremely rare. These findings suggest a choroidal origin of lymphomatous cells and hightlights the importance of macular OCT as a modality to enhance early detection and diagnosis of vitreo-retinal lymphoma.

ACKNOWLEDGEMENT/DISCOLOSURE

a. Funding/Support: This work was supported by the Research To Prevent Blindness Inc. (DS), New York NY and the Macula Foundation Inc. (DS, KBF), New York NY for the design and conduct of the study and the Cancer Center Support Grant (P30 CA008748) (F JH) for collection, management, analysis, and interpretation of the data.

b. Financial disclosures: R.D.M. is a consultant to Heidelberg Engineering, she receives research support from Allergan, Genentech/Roche, and Novartis; DS is a consultant to Amgen, Bayer, Genentech, Iveric bio, Novartis and Optovue and has received speaker fees from Optovue and research grants from Genentech, Heidelberg, Optovue, Regeneron and Topcon; K.B.F is a consultant to Genentech, Zeiss, Heidelberg Engineering, Allergan, Bayer, and Novartis. None of the other Authors have any other relationships or activities that readers could perceive to have influenced, or that give the appearance of potentially influencing what is written in the submitted work.

The principal investigator (Francesco Pichi) and the Senior Author (David Sarraf) had full access to all the data in the study and takes responsibility for the integrity of the data and the accuracy of the data analysis.

c. No Other Acknowledgments necessary.

REFERENCES

1. Davis JL. Intraocular lymphoma: a clinical perspective. Eye 2013; 27: 153–162.

2. Chan CC, Rubenstein JL, Coupland SE, et al. Primary vitreoretinal lymphoma: a report from an International Primary Central Nervous System Lymphoma Collaborative Group symposium. Oncologist 2011; 16: 1589–1599.

3. Chan CC, Sen HN. Current concepts in diagnosing and managing primary vitreoretinal (intraocular) lymphoma. Discov Med 2013;15:93–100.

4. Coupland SE, Chan CC, Smith J. Pathophysiology of retinal lymphoma. *Ocul Immunol Inflamm*. 2009;17:227–37.

5. Coupland SE, Heimann H, Bechrakis NE. Primary intraocular lymphoma: a review of the clinical, histopathological and molecular biological features. *Graefes Arch Clin Exp Ophthalmol* 2004;242(11):901–913.

6. DeAngelis LM. Primary central nervous system lymphoma. Recent Results Cancer Res 1994;135:155–169.

7. Hochberg FH, Miller DC. Primary central nervous system lymphoma. *J Neurosurg* 1988;68(6):835–853.

8. Peterson K, Gordon KB, Heineman MH, DeAngelis LM. The clinical spectrum of ocular lymphoma. *Cancer* 1993;72(3): 843–849.

9. Verbraeken HE, Hanssens M, Priem H, et al. Ocular non- Hodgkin's lymphoma: a clinical study of nine cases. *Br J Ophthalmol* 1997;81(1):31–36.

10. Grimm SA, Pulido JS, Jahnke K, et al. Primary intraocular lymphoma: an International Primary Central Nervous System Lymphoma Collaborative Group Report. *Ann Oncol*. 2007;18(11):1851-1855.

11. Fend F, Süsskind D, Deuter C, Coupland SE. Maligne Lymphome des Auges. *Pathologe*. 2017

12. Whitcup SM, de Smet MD, Rubin BI, et al. Intraocular lymphoma. Clinical and histopathologic diagnosis. *Ophthalmology*. 1993 Sep;100(9):1399-406.

13. Grimm SA, McCannel CA, Omuro AM, et al. Primary CNS lymphoma with intraocular involvement: International PCNSL Collaborative Group Report. *Neurology* 2008; 71(17):1355–1360.

14. Mochizuki M, Singh AD. Epidemiology and clinical features of intraocular lymphoma. *Ocul Immunol Inflamm* 2009;17(2):69–72.

15. Kimura K, Usui Y, Goto H. The Japanese intraocular lymphoma study group. Clinincal features and diagnostic significance of the intraocular fluid of 217 patients with intraocular lymphoma. *Jpn J Ophthalmol* 2012;56(4):383–389.
16. Mochizuki M, Singh AD. Epidemiology and clinical features of intraocular lymphoma. Ocul Immunol Inflamm 2009;17:69–72.
17. Coupland SE, Damato B. Understanding intraocular lymphomas. *Clin Experiment Ophthalmol* 2008;36:564–578.
18. Chan CC,Wallace DJ. Intraocular lymphoma: update on diagnosis and management. *Cancer Control* 2004;11:285–295.
19. Choi JY, Kafkala C, Foster CS. Primary intraocular lymphoma: a review. Semin Ophthalmol 2006;21:125–133. Review.
20. Rothova A, Ooijman F, Kerkhoff F, et al. Uveitis masquerade syndromes. *Ophthalmology* 2001;108:386–399.
21. Grange LK, Kouchouk A, Dalal MD, et al. Neoplastic masquerade syndromes in patients with uveitis. *Am J Ophthalmol* 2014;157:526–531.
22. Rajagopal R, Harbour JW. Diagnostic testing and treatment choices in primary vitreoretinal lymphoma. *Retina* 2011;31:435–440.
23. Forooghian F, Merkur AB, White VA, et al. High-definition optical coherence tomography features of primary vitreoretinal lymphoma. Ophthalmic Surg Lasers Imaging 2011;42:e97–99.
24. Velez G, Chan CC, Csaky KG. Fluorescein angiographic findings in primary intraocular lymphoma. *Retina* 2002;22:37–43.
25. Fardeau C, Lee CP, Merle-Béral H, et al. Retinal fluorescein, indocyanine green angiography, and optic coherence tomography in non-Hodgkin primary intraocular lymphoma. *Am J Ophthalmol* 2009;147:886–894.
26. Cassoux N, Merle-Beral H, Leblond V, et al. Ocular and central nervous system lymphoma: clinical features and diagnosis. *Ocul Immunol Inflamm*. 2000;8:243–50.
27. Velez G, Chan CC, Csaky KG. Fluorescein angiographic findings in primary intraocular lymphoma. Retina. 2002;22:37–43.
28. Turaka K, Bryan JS, De Souza S, et al. Vitreoretinal lymphoma: changing trends in diagnosis and local treatment modalities at a single institution. *Clin Lymphoma Myeloma Leuk*. 2012;12:412–7.

29. Kitao M, Hashida N, Nishida K. Recurrent pseudohypopyon in association with primary vitreoretinal lymphoma: a case report. *BMC Ophthalmol*. 2016;16:103.
30. Ishida T, Takase H, Arai A, Ohno-Matsui K. Multimodal imaging of secondary vitreoretinal lymphoma with optic neuritis and retinal vasculitis. *Am J Ophthalmol Case Rep*. 2020;18:100696.
31. Sagoo MS, Mehta H, Swampillai AJ, et al. Primary intraocular lymphoma. *Surv Ophthalmol* 2014;59:503–16.
32. Davis JL, Ruiz P Jr, Shah M, Mandelcorn ED. Evaluation of the reactive T-cell infiltrate in uveitis and intraocular lymphoma with flow cytometry of vitreous fluid (an American Ophthalmological Society thesis). *Trans Am Ophthalmol Soc*. 2012 Dec;110:117-29.
33. Bonzheim I, Giese S, Deuter C, et al. High frequency of MYD88 mutations in vitreoretinal B-cell lymphoma: a valuable tool to improve diagnostic yield of vitreous aspirates. *Blood*. 2015;126(1):76-79.
34. Yang X, Dalvin LA, Mazloumi M, et al. Spectral-Domain Optical Coherence Tomography Features of Vitreoretinal Lymphoma in 55 Eyes: Impact on Local Tumor Control. *Retina* 2020; in press.
35. Vasconcelos-Santos DV, De Puy E Souza GH, de Faria BB, et al. Subretinal pigment epithelial infiltrates in primary vitreoretinal lymphoma. *J Ophthalmic Inflamm Infect* 2011;1:171.
36. Dolz-Marco R, Gallego-Pinazo R, Jung JJ, et al. Sequential multimodal imaging findings in a case of primary vitreoretinal lymphoma. *Retin Cases Brief Rep* 2014;8:314–7.
37. Morara M, Foschi F, Veronese C, et al. Two cases of primary vitreoretinal lymphoma: a diagnostic challenge : The supporting role of multimodal imaging in the diagnosis of primary vitreoretinal lymphoma. *Int Ophthalmol*. 2018 Feb;38(1):353-361.
38. Saito T, Ohguro N, Iwahashi C, et al. Optical coherence tomography manifestations of primary vitreoretinal lymphoma. *Graefes Arch Clin Exp Ophthalmol* 2016;254:2319–26.
39. Pang CE, Shields CL, Jumper JM, Yannuzzi LA. Paraneoplastic cloudy vitelliform submaculopathy in primary vitreoretinal lymphoma. *Am J Ophthalmol*. 2014;158(6):1253-1261.e2
40. Barry RJ, Tasiopoulou A, Murray PI, et al. Characteristic optical coherence tomography findings in patients with primary vitreoretinal lymphoma: a novel aid to early diagnosis. *Br J Ophthalmol*. 2018;102(10):1362-1366.

41. Casady M, Faia L, Nazemzadeh M, Nussenblatt R, Chan CC, Sen HN. Fundus autofluorescence patterns in primary intraocular lymphoma. *Retina*. 2014;34(2):366-372.
42. Yang X, Dalvin LA, Mazloumi M, et al. SPECTRAL DOMAIN OPTICAL COHERENCE TOMOGRAPHY FEATURES OF VITREORETINAL LYMPHOMA IN 55 EYES. *Retina*. 2021 Feb 1;41(2):249-258.
43. Sood AB, Yeh S, Mendoza P, Grossniklaus HE. Histopathologic Diagnosis of Atypical Primary Vitreoretinal Lymphoma following Enucleation. *Ocul Oncol Pathol*. 2016 Oct;2(4):242-245.
44. Albadri ST, Pulido JS, Macon WR, Garcia JJ, Salomao DR. HISTOLOGIC FINDINGS IN VITREORETINAL LYMPHOMA: Learning From Enucleation Specimens. *Retina*. 2020 Feb;40(2):391-398.
45. Giannini C, Dogan A, Salomão DR. CNS lymphoma: a practical diagnostic approach. *J Neuropathol Exp Neurol*. 2014 Jun;73(6):478-94.
46. Kase S, Namba K, Kanno-Okada H, et al. Immunohistochemical and Immunocytochemical Analyses in Patients with Vitreoretinal Lymphoma. *Ocul Immunol Inflamm*. 2020;28(1):147-155.
47. Vasconcelos-Santos DV, De Puy E Souza GH, de Faria BB, et al. Subretinal pigment epithelial infiltrates in primary vitreoretinal lymphoma. *J Ophthalmic Inflamm Infect*. 2011 Dec;1(4):171.
48. Deák GG, Goldstein DA, Zhou M, Fawzi AA, Jampol LM. Vertical Hyperreflective Lesions on Optical Coherence Tomography in Vitreoretinal Lymphoma. *JAMA Ophthalmol*. 2019;137(2):194-198.
49. Chan CC, Shen D, Hackett JJ, Buggage RR, Tuaillon N. Expression of chemokine receptors, CXCR4 and CXCR5, and chemokines, BLC and SDF-1, in the eyes of patients with primary intraocular lymphoma. *Ophthalmology*. 2003 Feb;110(2):421-6.
50. Hilely A, Au A, Freund KB, et al. Non-neovascular age-related macular degeneration with subretinal fluid. *Br J Ophthalmol*. 2021 Oct;105(10):1415-1420.
51. Sharma A, Kumar N, Parachuri N, et al. Understanding the Mechanisms of Fluid Development in Age-Related Macular Degeneration. *Ophthalmol Retina*. 2021 Feb;5(2):105-107.

FIGURE CAPTIONS

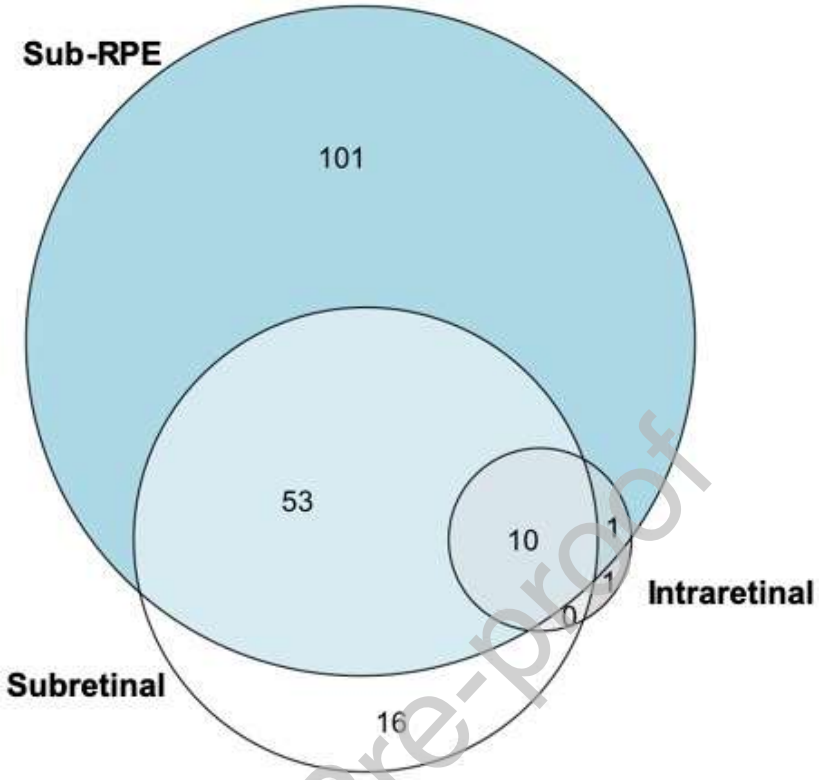

Figure 1. *Venn diagram illustrating baseline distribution of hyperreflective lymphomatous lesions across the various optical coherence tomography (OCT) retinal levels.*
In the 182 eyes with biopsy-proven vitreoretinal lymphoma studied with OCT analysis, sub-retinal pigment epithelium lymphomatous lesions were the most common finding (91%) followed by subretinal lesions (43%), while 12 eyes (7%) exhibited intraretinal involvement. Isolated sub-RPE infiltrates (55%) or combined sub-RPE and subretinal infiltrates (29%) represented the most common baseline presentations. Ten eyes (5%) illustrated lesions at all 3 levels at baseline. Isolated intraretinal lesions were extremely rare.

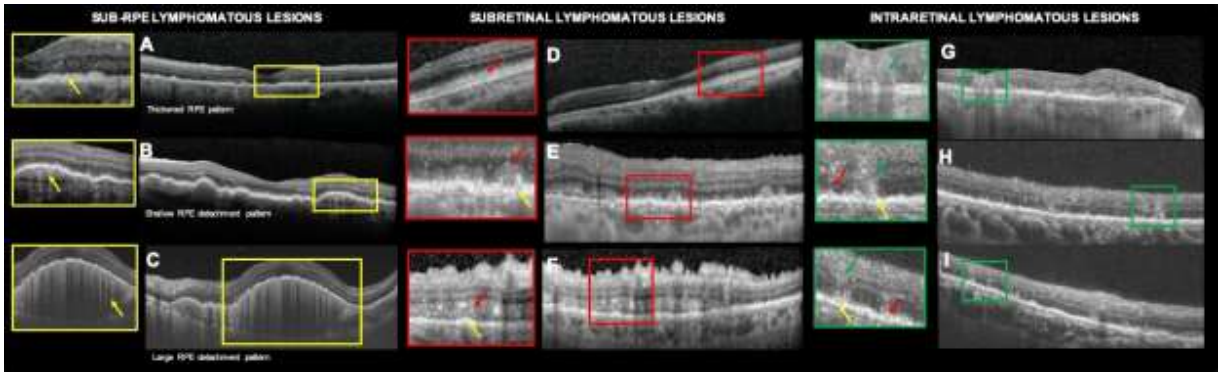

Figure 2. *Optical coherence tomography illustrating hyperreflective lymphomatous lesions in all 3 retinal spaces.*

In this study, hyperreflective lesions in patients with vitreoretinal lymphoma were most commonly identified in the sub-retinal pigment epithelium (RPE) space (A,B,C), but were also present in the subretinal space (D,E,F) and in some cases were identified in the inner and/or outer retina (G,H,I). Sub-RPE lesions displayed 3 morphological sub-types with OCT. The most common, a "thickened RPE pattern" (A, yellow arrow) was usually associated with concomitant lesions in the subretinal (E,F, yellow arrows) and intraretinal (G,H,I, yellow arrows) compartments. The "shallow retinal pigment epithelium detachment" sub-type (B, yellow arrow) and the "large retinal pigment epithelium detachment" sub-type (C, yellow arrow) were more rarely associated with hyperreflective lesions in the subretinal space. Subretinal lesions either extended horizontally in a band-like pattern under the retina (D,F, red arrows) or displayed a focal round hyperreflective pattern (E, red arrow) and were more commonly seen in association with intraretinal lesions (H,I, red arrows).

Intraretinal extension of the hyperreflective lymphomatous lesions (G,H,I, green arrows) were very rarely isolated and were almost always identified in association with sub-retinal pigment epithelium and subretinal lesions.

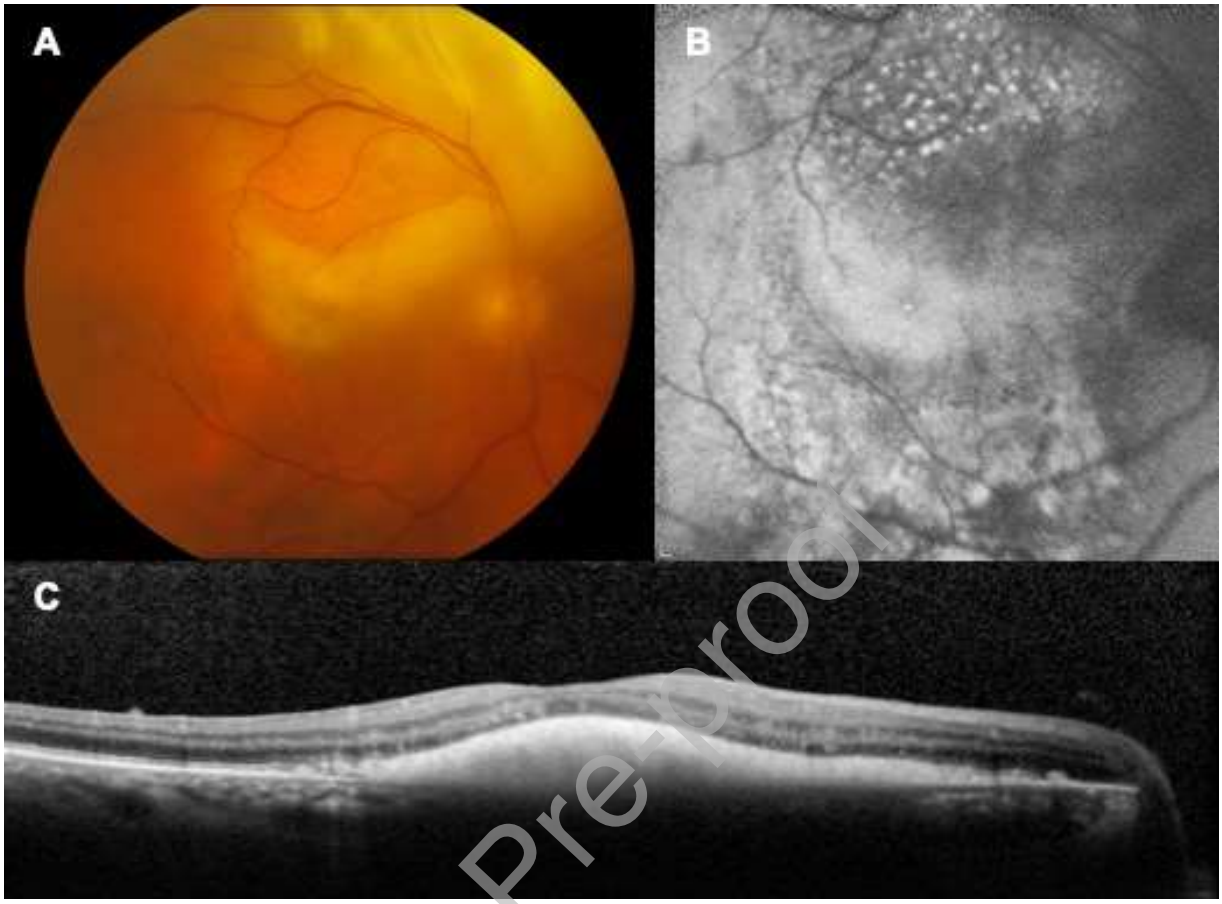

Figure 3. *Multimodal imaging of a case of cloudy vitelliform maculopathy associated with vitreoretinal lymphoma (VRL).*

Color fundus photography of the right eye (A) illustrates cloudy creamy yellow submacular material with extensions along the superior arcade and multiple, small, punctate yellow-white spots scattered superior to the macula. Fundus autofluorescence shows low-intensity hyperautofluorescence of the cloudy vitelliform submacular lesion with speckled hyperautofluorescence in the superior macula. Spectral-domain optical coherence tomography through the fovea illustrates the dense hyperreflective subretinal material above the RPE band which can be highly suggestive of VRL but was present in only 9% of our cohort.

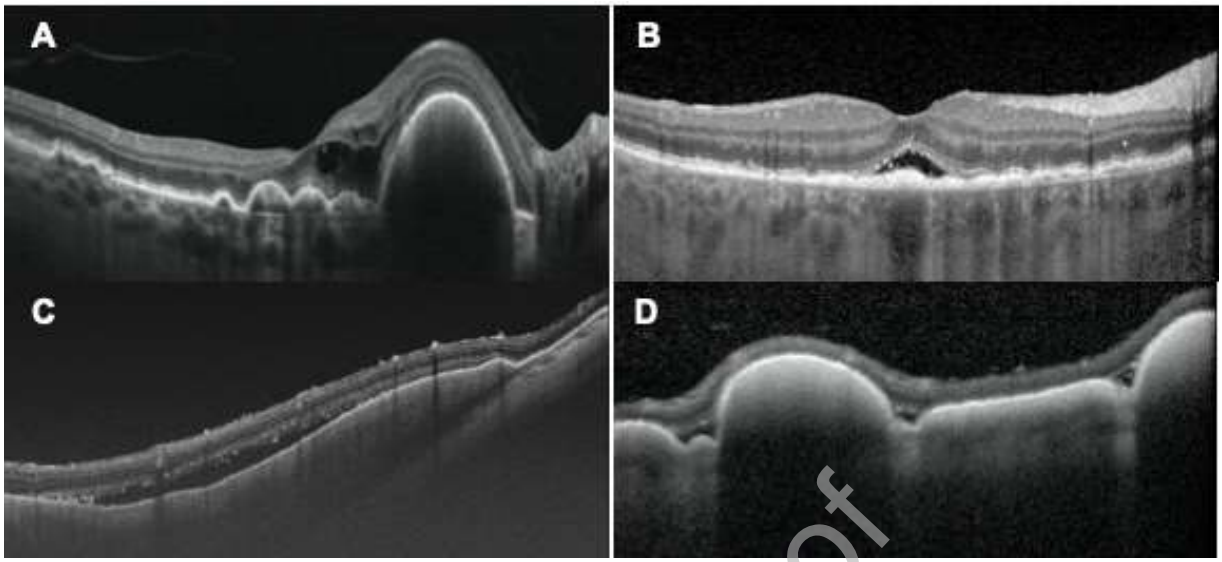

Figure 4. *Optical coherence tomography (OCT) showing intraretinal and subretinal fluid in cases of vitreo-retinal lymphoma.*

Note the presence of intraretinal fluid (A), observed in 13% of eyes with vitreoretinal lymphoma, and subretinal fluid (B,C,D), identified in 11% of eyes in this study. Subretinal fluid was most commonly associated with sub-retinal pigment epithelium lesions (B,C,D), especially with large RPE detachments (B,D), that may be secondary to impairment of the retinal pigment epithelium pumping capacity especially when the RPE is further displaced from the underlying choroid.

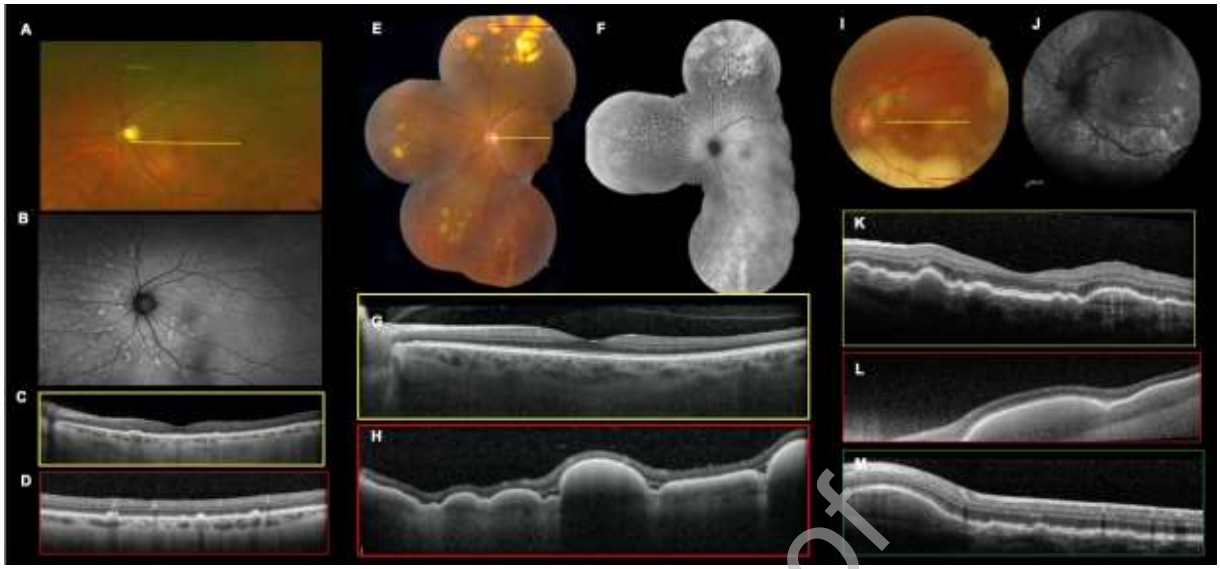

Figure 5. *Multimodal imaging of 3 patients with vitreo-retinal lymphoma.*
Corresponding color fundus photograph, fundus autofluorescence and spectral domain OCT are illustrated for all 3 cases (A-D, E-H, and I-M). The level of the corresponding OCT is indicated by the colored line in the fundus photograph. Fundus photographs in patients with vitreo-retinal lymphoma illustrate extra-macular (A, E) and macular (I) lesions either in the form of mild retinal pigment epithelium mottling (A) or as discrete sub-retinal pigment epithelium lesions (E, I). The most common fundus autofluorescence finding of vitreo-retinal lymphoma was hyperautofluorescence in the form of a "leopard spot" pattern (B, F) which strongly correlated with hyperreflective "thickened retinal pigment epithelium" lesions on optical coherence tomography (C, D). The "large retinal pigment epithelium detachment" pattern noted with optical coherence tomography (H) typically illustrated a diffuse and homogeneous hyperautofluorescence (F) with fundus autofluorescence, while "shallow RPE detachments" of lymphomatous material (K-M) were associated with faint hypoautofluorescence (J).

Table 1. Demographic, ocular and tomographic features of 182 eyes of 115 patients with biopsy proven vitreoretinal lymphoma.

Demographic N = 115 Patients (%)		
Sex		
Male		52 (45)
Female		63 (55)
Race		
Caucasian		97 (84)
African American		7 (6)
Asian		7 (6)
Indian		4 (3)
Age at presentation (y)		
Mean (range)		65 (25-91)
Systemic lymphoma		
Central nervous system lymphoma		54 (47)
Non-central nervous system lymphoma		11 (10)
Both		12 (10)
Ocular Features N = 182 Eyes (%)		
Laterality (n = patients)		
Unilateral		48 (26)
Bilateral		134 (74)
Visual acuity (Snellen), mean		20/30
Visual acuity (LogMAR), mean		0.2
SD-OCT Features N = 182 Eyes (%)		
Intraretinal deposits		1 (0.5)
Subretinal deposits		16 (9)
Sub-RPE deposits		101 (55)
Thickened RPE		89 (49)
Shallow PED		39 (21)
Large PED		37 (20)
Intraretinal + Subretinal deposits		0 (0)
Intraretinal + Sub-RPE deposits		1 (0.5)
Subretinal + Sub-RPE deposits		53 (29)
Intraretinal + Subretinal + Sub-RPE deposits		10 (5)

Dr Francesco Pichi is a retina and uveitis specialist at Cleveland Clinic Abu Dhabi and is Director of the Ophthalmology Residency Program. Dr Pichi has to his credit more than 100 presentations in both international and national conferences and 100 peer reviewed publications. He has authored 12 chapters in various text books and published a book on “Complications in uveitis”. He currently resides in Abu Dhabi and is an avid rock climber.